

## A NOTE ON THE LASOTA DISCRETE MODEL FOR BLOOD CELL PRODUCTION

EDUARDO LIZ

Departamento de Matemática Aplicada II, Universidade de Vigo  
36310 Vigo, Spain

CRISTINA LOIS-PRADOS

Instituto de Matemáticas, Universidade de Santiago de Compostela  
Campus Vida, 15782 Santiago de Compostela, Spain

*Dedicated to Prof. Juan J. Nieto on the occasion of his 60th birthday*

**ABSTRACT.** In an attempt to explain experimental evidence of chaotic oscillations in blood cell population, A. Lasota suggested in 1977 a discrete-time one-dimensional model for the production of blood cells, and he showed that this equation allows to model the behavior of blood cell population in many clinical cases. Our main aim in this note is to carry out a detailed study of Lasota's equation, in particular revisiting the results in the original paper and showing new interesting phenomena. The considered equation is also suitable to model the dynamics of populations with discrete reproductive seasons, adult survivorship, overcompensating density dependence, and Allee effects. In this context, our results show the rich dynamics of this type of models and point out the subtle interplay between adult survivorship rates and strength of density dependence (including Allee effects).

**1. Introduction.** Based on experimental results, the Polish mathematician Andrzej Lasota proposed in 1977 [5] a discrete model for the production of red blood cells (erythrocytes). If  $x_n$  denotes the number of cells at time  $n$ , and  $\sigma x_n$  is the number of cells destroyed in the time interval  $[n, n + 1]$ , then the dynamics is governed by equation

$$x_{n+1} - x_n = -\sigma x_n + p_n, \quad (1.1)$$

where  $p_n$  is the number of cells which are produced in the bone marrow during the same period. The bone marrow has the ability to change production when the number of blood cells changes, so  $p_n = p(x_n)$ . Based on experimental results, the form  $p(x) = (cx)^\gamma e^{-x}$  was proposed for the production function, thus leading to the difference equation

$$x_{n+1} = (1 - \sigma)x_n + (cx_n)^\gamma e^{-x_n}, \quad (1.2)$$

where  $\sigma \in (0, 1)$  and  $c, \gamma$  are positive constants.

As indicated by Lasota, equation (1.2) provides a flexible model that explains the behavior of the blood cell population in many clinical cases. For example, if  $\gamma > 1$ , then there is a critical value of the population size such that populations

---

2010 *Mathematics Subject Classification.* 39A10, 39A30, 92C37, 92D25.

*Key words and phrases.* Discrete-time model, gamma model, Ricker map, stability, bifurcations, boundary collision, essential extinction.

below it cannot survive in the long term. In population dynamics, such effect is known as a strong Allee effect [4]. In the model under consideration, it means that if the number of cells is too small (for example, after a heavy hemorrhage), then the organism eventually dies. Cell populations above the critical value usually persist and they can approach a stable positive equilibrium (which is considered the normal behavior), but the number can oscillate when there is a disease affecting the blood cell production, and even behave in an erratic (aperiodic) way in the case of a severe disease. As the examples in [5] show, an increasing value of  $\sigma$  leads to severe disease (because a large proportion of cells are destroyed). Even though this model assumes that the blood production is not a continuous process (a more accurate model seems to be a delay differential equation [5, 16]), it is quite intuitive and displays a very rich dynamics.

On the other hand, equation (1.2) can also be considered as a discrete model for iteroparous populations (that is, part of the population survives the reproductive season) whose recruitment function is defined by a gamma-Ricker map [8]. In this context, equation (1.2) is a flexible model for populations with discrete reproductive seasons, adult survivorship, overcompensating density dependence, and Allee effects.

In this note, we show some interesting aspects of the dynamics of (1.2) that can help to understand the potential effects of increasing either the destruction rate of cells (in the erythropoietic model), or the adult mortality rate (in the population model).

**2. Preliminary results.** We first introduce the maps  $f : [0, \infty) \rightarrow [0, \infty)$  and  $F : [0, \infty) \rightarrow [0, \infty)$  defined by

$$f(x) = (cx)^\gamma e^{-x}, \quad F(x) = (1 - \sigma)x + (cx)^\gamma e^{-x} = (1 - \sigma)x + f(x), \quad (2.1)$$

where  $\sigma \in (0, 1)$ ,  $c, \gamma > 0$ . Notice that equation (1.2) can be written in the form  $x_{n+1} = F(x_n)$ .

Some properties of the map  $f$  have been recently proved in [8], and they will be useful in our analysis. Now, we state the intervals of monotonicity of  $F$  depending on the parameters. We prove that  $F$  can be either increasing or bimodal (see Figure 2.1).

**Theorem 2.1.** *The map  $F$  defined in (2.1) has the following properties:*

- (a):  $F(0) = 0$  and  $\lim_{x \rightarrow \infty} F(x) = \infty$ .
- (b):  $F$  is differentiable in  $(0, \infty)$ ,  $F'(0^+) = 1 - \sigma$  if  $\gamma > 1$ ,  $F'(0^+) = 1 - \sigma + c$  if  $\gamma = 1$ , and  $F'(0^+) = \infty$  if  $0 < \gamma < 1$ . In any case,  $\lim_{x \rightarrow \infty} F'(x) = 1 - \sigma > 0$ .
- (c): Define  $H(\gamma) = \sqrt{\gamma}(\gamma + \sqrt{\gamma})^{\gamma-1} e^{-\gamma-\sqrt{\gamma}}$ .
  - (i) If  $c^\gamma H(\gamma) < 1$  and  $0 < \sigma \leq \sigma^* := 1 - c^\gamma H(\gamma)$ , then  $F$  is increasing in  $(0, \infty)$ .
  - (ii) If  $c^\gamma H(\gamma) \geq 1$ , or  $c^\gamma H(\gamma) < 1$  and  $\sigma > \sigma^*$ , then  $F$  has two positive critical points  $c_1 < c_2$ . Moreover,  $F$  attains a local maximum at  $c_1$  and a local minimum at  $c_2$ .

*Proof.* The proof of items (a) and (b) is elementary, so we only provide the proof of (c).

The first and second derivatives of  $F$  in  $(0, \infty)$  are

$$F'(x) = (1 - \sigma) + c^\gamma x^{\gamma-1} e^{-x} (\gamma - x),$$

$$F''(x) = c^\gamma e^{-x} x^{\gamma-2} (x^2 - 2\gamma x + \gamma^2 - \gamma).$$

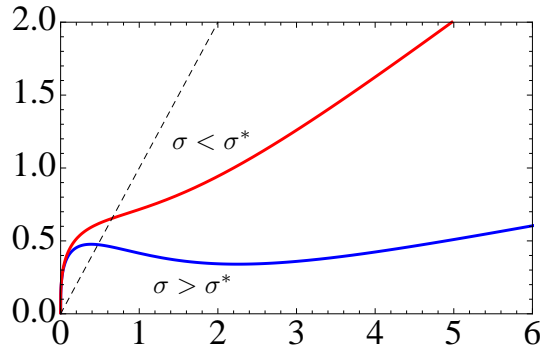


FIGURE 2.1. Graphs of the map  $F$  for  $\gamma = 0.3$ ,  $c = 0.6$ , and different values of  $\sigma$ :  $\sigma = 0.6 < \sigma^* \approx 0.774$  in red ( $F$  is increasing), and  $\sigma = 0.9 > \sigma^*$  in blue ( $F$  has two critical points). The dashed line is the graph of  $y = x$ .

We distinguish two cases according to the zeros of  $F''$  on  $(0, \infty)$  (see Figure 2.2).

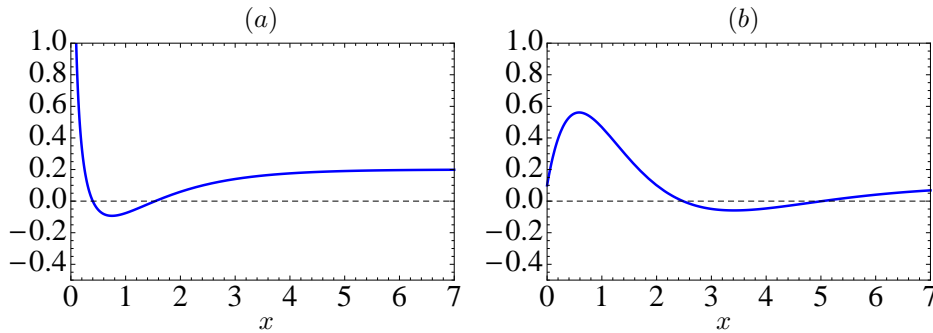


FIGURE 2.2. Graphs of the map  $F'$  (solid, blue) and the line  $y = 0$  (dashed, black), with  $c=1$ . (a):  $\gamma = 0.25 < 1$ ,  $\sigma = 0.8 > \sigma^* \approx 0.707$ ; (b):  $\gamma = 2 > 1$ ,  $\sigma = 0.9 > \sigma^* \approx 0.841$ . In both cases, there are two intersection points, that determine the critical points of  $F$ .

If  $\gamma \leq 1$ , then  $F'$  has a unique critical point at  $d^+ = \gamma + \sqrt{\gamma}$ ; moreover,  $F'$  is decreasing on  $(0, d^+)$  and increasing on  $(d^+, \infty)$ .

If  $\gamma > 1$ , then  $F''(d^+) = F''(d^-) = 0$ , where  $d^+ = \gamma + \sqrt{\gamma} > d^- = \gamma - \sqrt{\gamma} > 0$ . In this case,  $F'(0^+) > 0$ ,  $F'$  is increasing on  $(0, d^-) \cup (d^+, \infty)$ , and decreasing on  $(d^-, d^+)$ .

In both cases, it is clear that  $F'(x) \geq 0$  for all  $x > 0$  if and only if  $F'(d^+) \geq 0$ , and  $F'$  has two positive zeros  $c_1 < c_2$  if  $F'(d^+) < 0$ . Moreover, it follows from the sign of  $F'$  that  $c_1$  corresponds to a local maximum of  $F$ , and  $c_2$  to a local minimum.

Finally, it is easy to check that condition  $F'(\gamma + \sqrt{\gamma}) \geq 0$  is equivalent to  $\sigma \leq 1 - c^\gamma H(\gamma)$ . □

**3. Fixed points and stability.** We first address the case  $0 < \gamma \leq 1$ , for which the map  $F$  can have at most one positive equilibrium.

**Theorem 3.1.** Assume that  $0 < \gamma \leq 1$ .

- (a): If  $\gamma < 1$ , then  $F$  has a unique positive fixed point  $p$ . Moreover,  $F(x) > x$  if  $0 < x < p$ , and  $F(x) < x$  if  $x > p$ .
- (b): If  $\gamma = 1$ , then  $F$  has a unique positive fixed point  $p$  if  $c > \sigma$  and no positive fixed points if  $c \leq \sigma$ . In the former case,  $F(x) > x$  if  $0 < x < p$ , and  $F(x) < x$  if  $x > p$ .
- (c): Assume that  $0 < \gamma < 1$ , or  $\gamma = 1$  and  $c > \sigma$ . Then the unique positive equilibrium  $p$  is locally asymptotically stable for the Lasota equation (1.2) if the following condition holds:

$$c^\gamma < G(\gamma, \sigma) := \sigma \left( \gamma + \frac{2}{\sigma} - 1 \right)^{1-\gamma} e^{\gamma + \frac{2}{\sigma} - 1}. \quad (3.1)$$

If  $c^\gamma > G(\gamma, \sigma)$ , then  $p$  is unstable.

*Proof.* We only prove the case  $\gamma < 1$ , since the proof for  $\gamma = 1$  is very similar.

The fixed point  $p > 0$  satisfies the identity

$$f_1(p) := \sigma p^{1-\gamma} = c^\gamma e^{-p} =: f_2(p).$$

The existence and uniqueness of  $p$  follows from the fact that  $f_1(x) = \sigma x^{1-\gamma}$  is increasing, with  $f_1(0) = 0$ , and  $f_2(x) = c^\gamma e^{-x}$  is decreasing, with  $f_2(0) > 0$ ,  $f_2(\infty) = 0$ . A simple graphical analysis shows that  $F(x) > x$  if  $0 < x < p$ , and  $F(x) < x$  if  $x > p$ .

The derivative of  $F$  at the fixed point  $p$  is

$$F'(p) = 1 - \sigma + \gamma c^\gamma p^{\gamma-1} e^{-p} - c^\gamma p^\gamma e^{-p} = 1 + \sigma(\gamma - 1 - p). \quad (3.2)$$

Since  $\gamma < 1$ , it is clear that  $F'(p) < 1$ . On the other hand, it follows from (3.2) that

$$F'(p) > -1 \iff p < \gamma + \frac{2}{\sigma} - 1.$$

Using the statement in (a), it is clear that the last inequality holds if and only if

$$F \left( \gamma + \frac{2}{\sigma} - 1 \right) < \gamma + \frac{2}{\sigma} - 1,$$

and this inequality is equivalent to (3.1).  $\square$

**Remark 3.2.** We notice that equation (1.2) is *uniformly permanent* if either  $\gamma < 1$  or  $\gamma = 1$  and  $\sigma < c$ . This means that there exists a compact interval  $[A, B]$  such that  $0 < A \leq \liminf_{n \rightarrow \infty} F^n(x) \leq \limsup_{n \rightarrow \infty} F^n(x) \leq B$ , for all  $x > 0$ . Indeed, if  $F$  is increasing then the unique positive equilibrium  $p$  is a global attractor, and we can choose  $A = B = p$ ; if  $F$  is bimodal, then elementary arguments show that we can choose  $A = F(c_2)$ ,  $B = F(c_1)$ , where  $c_1, c_2$  are the critical points of  $F$  ( $0 < c_1 < c_2$ ).

Next, if  $\gamma > 1$ , then  $F$  can have 0, 1, or 2 positive fixed points. This case is studied in our next result.

**Theorem 3.3.** Assume that  $\gamma > 1$ , and define

$$c^* := \left( \sigma(\gamma - 1)^{1-\gamma} e^{\gamma-1} \right)^{1/\gamma}. \quad (3.3)$$

Then the map  $F$  defined in (2.1) has two positive fixed points if  $c > c^*$ , one positive fixed point if  $c = c^*$ , and no positive fixed points if  $c < c^*$ . If  $F$  has only one fixed point  $q$ , then  $q = \gamma - 1$ ,  $F'(q) = 1$  and  $q$  is semi-stable. If  $F$  has two positive fixed

points  $q, p$ , then  $q < \gamma - 1 < p$ ,  $F'(q) > 1$ , and  $F'(p) < 1$ . The fixed point  $q$  is unstable, while  $p$  is asymptotically stable if (3.1) holds. If  $c < c^*$ , then all solutions of (1.2) converge to 0.

*Proof.* The positive fixed points of  $F$  are the solutions of equation  $f_1(x) = f_2(x)$ , where  $f_1(x) = \sigma x^{1-\gamma}$  and  $f_2(x) = c^\gamma e^{-x}$ . Since  $f_1(0^+) = \infty$ ,  $f_2(0) = c^\gamma$ ,  $f_1$  and  $f_2$  are decreasing and convex, and  $\lim_{x \rightarrow \infty} (f_1(x)/f_2(x)) = \infty$ , it follows from elementary arguments that  $F$  can have at most two positive fixed points.

Assume that there is at least one positive fixed point of  $F$ , and denote by  $q$  the smallest one. It follows from the properties of  $f_1$  and  $f_2$  that  $f'_1(q) \leq f'_2(q)$ . This inequality, together with the equality  $f_1(q) = f_2(q)$ , leads to  $q \leq \gamma - 1$ . If  $q = \gamma - 1$ , then  $f'_1(q) = f'_2(q)$  and  $\gamma - 1$  is the unique positive fixed point of  $F$ . However, if  $q < \gamma - 1$ , then  $f'_1(q) < f'_2(q)$ . Since  $\lim_{x \rightarrow \infty} (f_1(x)/f_2(x)) = \infty$ , there exists another fixed point  $p > q$ . Moreover,  $f'_1(p) > f'_2(p)$ , which is equivalent to  $p > \gamma - 1$ .

Thus:

- there is a unique positive fixed point of  $F$  if and only if  $q = \gamma - 1$ , that is, if  $f_1(\gamma - 1) = f_2(\gamma - 1)$ . This equality is equivalent to  $c = c^*$ ;
- there are two positive fixed points  $q, p$  of  $F$  if and only if  $f_1(\gamma - 1) < f_2(\gamma - 1)$ , which is equivalent to  $c > c^*$ ;
- $F$  does not have positive fixed points if  $c < c^*$ .

In the first case, it is easy to check that solutions of (1.2) starting at an initial condition  $x_0 \in (0, q)$  converge to zero. If  $F(x) \geq q$  for all  $x > q$ , then all solutions starting at  $[q, \infty)$  converge to  $q$ ; if there are points  $x > q$  such that  $F(x) < q$ , then the immediate basin of attraction of  $q$  is  $[q, r]$ , where  $r$  is the smallest point in  $F^{-1}(q) \setminus \{q\}$ . Therefore,  $q$  is semistable.

In the second case, we have that  $F'(p) < 1 < F'(q)$ . Thus,  $q$  is unstable. If (3.1) holds, then  $F'(p) > -1$ , implying that the equilibrium  $p$  is asymptotically stable.

Finally, if  $c < c^*$ , then  $F(x) < x$  for all  $x > 0$  and therefore all solutions of (1.2) converge to 0. □

Figure 3.1 shows the three different possibilities considered in the statement of Theorem 3.3.

It is well known that a discrete dynamical system generated by a map with two critical points can lead to the coexistence of several attractors. However, if  $\gamma < 1$  or  $\gamma = 1$  and  $\sigma < c$ , we will prove that the unique positive fixed point  $p$  is a global attractor of all positive solutions of (1.2) when it is asymptotically stable. Moreover, we get that the parameter region of global asymptotic stability includes the nonhyperbolic case, thus extending condition (3.1) to  $c^\gamma \leq G(\gamma, \sigma)$ .

To prove this result, we need the following generalization of Theorem 1 in [10].

**Theorem 3.4.** *Assume that  $0 < \sigma < 1$  and  $f : [0, \infty) \rightarrow [0, \infty)$  satisfies the following conditions:*

- (A1):  $g(x) = (1/\sigma)f(x)$  has a unique positive fixed point  $p > 0$ ,  $g(0) = 0$ , and  $g'(0^+) > 1$  ( $g'(0^+)$  can be  $\infty$ ).
- (A2):  $f$  has a unique critical point  $z$ ; moreover,  $f'(x) > 0$  for all  $x \in (0, z)$  and  $f'(x) < 0$  for all  $x > z$ .
- (A3):  $(Sf)(x) < 0$  for all  $x > z$ , where

$$(Sf)(x) = \frac{f'''(x)}{f'(x)} - \frac{3}{2} \left( \frac{f''(x)}{f'(x)} \right)^2$$

is the Schwarzian derivative of  $f$ .

**(A4):**  $f''(x) < 0$  for all  $x \in (0, z)$ .

Then, the unique positive equilibrium  $p$  of equation

$$x_{n+1} = (1 - \sigma)x_n + f(x_n) \quad (3.4)$$

is globally asymptotically stable if

$$1 - \sigma + f'(p) \geq -1. \quad (3.5)$$

If (3.5) does not hold, then  $p$  is unstable.

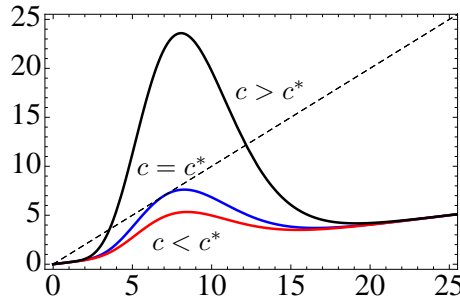


FIGURE 3.1. Graphs of the map  $F$  for  $\gamma = 8$ ,  $\sigma = 0.8$ , and different values of  $c$ :  $c = c^* \approx 0.425$  in blue (one positive fixed point),  $c = 0.4 < c^*$  in red (no positive fixed points), and  $c = 0.5 > c^*$  in black (two positive fixed points). The dashed line is the graph of  $y = x$ .

*Proof.* Equation (3.4) can be written in the form of equation (4) in [10]:

$$x_{n+1} = \alpha x_n + (1 - \alpha)g(x_n), \quad (3.6)$$

with  $\alpha = 1 - \sigma$  and  $g(x) = (1/\sigma)f(x)$ .

It is clear that conditions **(A2)**–**(A4)** hold for  $g$  because  $g'(x) = (1/\sigma)f'(x)$ ,  $g''(x) = (1/\sigma)f''(x)$ , and  $(Sg)(x) = (Sf)(x)$ .

There are two relevant differences with Theorem 1 in [10]. On the one hand, condition **(A3)** there required  $(Sf)(x) < 0$  for all  $x \neq z$ . However, a simple inspection of the proof shows that the less restrictive condition  $(Sf)(x) < 0$  for all  $x > z$  is enough to get the result. On the other hand, the restriction  $z < p$  is required in [10, Theorem 1]. In case  $z \geq p$ , the map  $\phi(x) = (1 - \sigma)x + f(x)$  defining the right-hand side of (3.4) satisfies  $\phi'(x) > 0$  for  $0 < x \leq p$ ,  $\phi(x) > x$  for  $x < p$ , and  $0 < \phi(x) < x$  for  $x > p$ . Hence, simple arguments show that  $p$  is globally asymptotically stable (see, e.g., [3, Lemma 1]).  $\square$

Now we are in a position to prove the global stability result for (1.2).

**Corollary 3.5.** *Assume that  $0 < \gamma < 1$ , or  $\gamma = 1$  and  $c > \sigma$ . Then, the unique positive equilibrium  $p$  for the Lasota equation (1.2) is globally asymptotically stable if and only if  $c^\gamma \leq G(\gamma, \sigma)$ , where  $G(\gamma, \sigma)$  is defined in (3.1).*

*Proof.* Consider the map  $f(x) = (cx)^\gamma e^{-x}$  defined in (2.1). It is clear from the proof of Theorem 3.1 that condition  $c^\gamma \leq G(\gamma, \sigma)$  is equivalent to (3.5). Thus, in order to use Theorem 3.4, we only need to check conditions **(A1)**–**(A4)**.

Conditions **(A1)** and **(A2)** follow from elementary arguments, and **(A3)** was proved in [8, Proposition 2]. Hence, it remains to prove **(A4)**.

From the proof of Theorem 2.1, we know that  $f''(x) < 0$  for all  $x \in (0, \gamma + \sqrt{\gamma})$ . Since the unique critical point of  $f$  is  $z = \gamma < \gamma + \sqrt{\gamma}$ , **(A4)** follows.  $\square$

**4. Dynamics and bifurcations.** In this section, we combine the rigorous analysis from the previous sections with numerical bifurcation diagrams to show the potential rich dynamics of the solutions to the Lasota equation (1.2) and the role of the parameters  $\gamma$  and  $\sigma$ . For parameter  $c$ , we fix the value  $c = 0.47$  already used by Lasota in [5]. Although his study is restricted to  $\gamma = 8$  and three different values of  $\sigma$  ( $\sigma = 0.1, 0.4, 0.8$ ), we will consider more cases to give an idea of the more relevant dynamical phenomena. In particular, we will revisit the cases studied by Lasota.

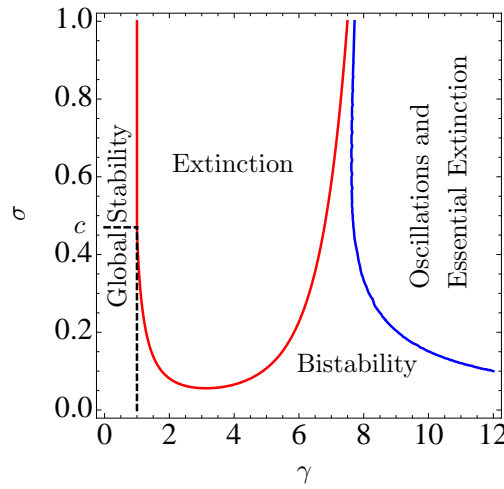


FIGURE 4.1. Main bifurcation boundaries and regions with different dynamical behavior for equation (1.2) with  $c = 0.47$ , in the parameter plane  $(\gamma, \sigma)$ . The two solid lines represent the extinction boundary (red color) and the stability boundary of the largest positive equilibrium (blue color). The vertical dashed line  $\gamma = 1$  (from  $\sigma = 0$  to  $\sigma = c = 0.47$ ) is the border between global stability of the unique positive equilibrium and a bistability region, in which both the largest positive equilibrium and the extinction equilibrium are asymptotically stable.

We begin by displaying in Figure 4.1 a bifurcation diagram for  $c = 0.47$ , which shows in the parameter plane  $(\gamma, \sigma)$  the stability and extinction boundaries provided in Section 3. In this case, condition  $c^\gamma \leq G(\gamma, \sigma)$  holds for all  $\gamma \in (0, 1]$ , and therefore Corollary 3.5 implies that the unique positive equilibrium is globally asymptotically stable in this parameter range (if  $\gamma = 1$ , this equilibrium exists only for  $\sigma < 0.47 = c$ ).

The red solid line is given by equation (3.3) when  $\gamma > 1$ . According to Theorem 3.3, this line corresponds to a tangent bifurcation and represents the boundary between extinction and bistability. In the bistable case, there are solutions that converge to the extinction equilibrium and others that converge to the largest positive

equilibrium, so permanence depends on the initial condition. For  $\sigma > c$ , the red line  $\gamma = 1$  represents the boundary between global stability of the positive equilibrium and extinction.

The blue solid line represents the boundary of local asymptotic stability of  $p$ , so the region to the right of this line corresponds to more complicated dynamics, which includes periodic attractors, chaotic attractors, and essential extinction, as we show below in some numerical bifurcation diagrams. We recall that essential extinction means that almost all solutions (in a sense of Lebesgue measure) converge to zero [14, 15]. Essential extinction usually occurs after a boundary collision between the basins of attraction of a chaotic attractor and the extinction equilibrium 0; however, we report below different transitions from bistability to essential extinction.

In the remainder of this section, we show some relevant numerical bifurcation diagrams to illustrate the rich behavior of equation (1.2). The value of  $c$  is always set to 0.47. In some cases (Figures 4.2, 4.3), we fix a value of  $\gamma$  and use  $\sigma$  as a bifurcation parameter, while in Figure 4.4 we do the opposite.

**4.1. Bubbles.** A first interesting phenomenon is the existence of the so-called *bubbles*, which are characteristic in bifurcation diagrams of population models where some adults survive more than one reproduction period. A primary bubble in the sense of [11, Definition 3] is shown in Figure 4.2: the largest positive equilibrium loses its asymptotic stability in a period-doubling bifurcation as the destruction rate  $\sigma$  is increased, but stability is regained at a larger value of  $\sigma$ , after a period-halving bifurcation occurs. This phenomenon shows that increasing the mortality rate can be either stabilizing or destabilizing. More complex bubbling effects can be observed in Figure 4.3 (c). In this case, the equation can reach a chaotic regime inside the bubble (see [11] for more details and related references).

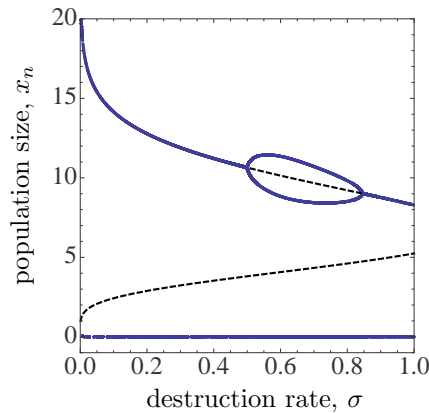


FIGURE 4.2. Bifurcation diagram showing a bubble for equation (1.2) with  $c = 0.47$ ,  $\gamma = 7.65$ , using  $\sigma$  as the bifurcation parameter. Black dashed lines correspond to unstable equilibria.

**4.2. Hydra effect.** It is easy to check that the largest equilibrium of (1.2) decreases as  $\sigma$  is increased. However, the average population size of the nontrivial attractor can increase with  $\sigma$  when the largest equilibrium loses its asymptotic stability. This phenomenon can be observed in Figure 4.3 (b), where the average of the



2-periodic attractor is represented by a solid red line. The phenomenon of a population increasing in response to an increase in its per-capita mortality rate is known as the hydra effect [1]. A formal notion of hydra effect suitable for the context of this paper is given in [11, Definition 2].

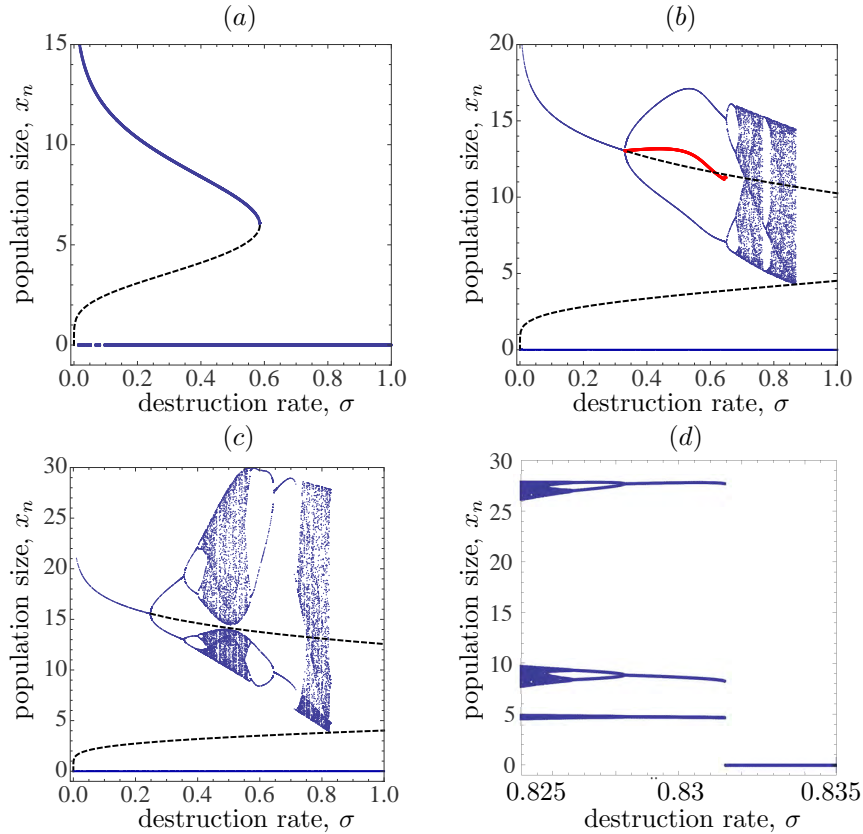


FIGURE 4.3. Bifurcation diagrams for equation (1.2) with  $c = 0.47$ , using  $\sigma$  as the bifurcation parameter. Black dashed lines correspond to unstable equilibria. For more details, see the text. (a):  $\gamma = 7$ ; (b):  $\gamma = 8$ ; (c):  $\gamma = 8.5$  and  $\sigma \in (0, 1)$ ; (d): magnification for  $\gamma = 8.5$ .

**4.3. Sudden collapses.** A typical feature of population models with Allee effects, where population cannot survive in the long term if its abundance is below a critical size, is the possibility of sudden collapses. Roughly speaking, this means that there are critical values of some relevant parameter such that extinction occurs if the parameter goes beyond this critical value, while populations can persist at densities bounded away from zero for values just below the critical one. Sudden collapses typically occur when the basins of attraction of the zero equilibrium and another attractor collide (boundary collisions). See, e.g., [6, 14, 15].

There are two main mechanisms leading to sudden collapses. The simplest one is a tangent bifurcation, which leads from bistability to extinction when the two positive equilibria of (1.2) collide and then disappear (see Figure 3.1). A bifurcation

diagram showing this first case is given in Figure 4.3 (a), for  $c = 0.47$  and  $\gamma = 7$ . A more complex mechanism for sudden collapses is a catastrophe bifurcation, which takes place when a chaotic attractor collides with the basin of attraction of zero. This situation is represented in Figure 4.3 (b), for  $c = 0.47$  and  $\gamma = 8$ . We emphasize that these are the values chosen by Lasota [5] to investigate the dynamics of (1.2) as  $\sigma$  is increased. Although he found chaotic orbits for  $\sigma = 0.8$ , it seems he did not observe the sudden collapse, which occurs at  $\sigma \approx 0.87$ , when  $F^2(c_1) = q$ . As before,  $c_1$  and  $q$  are the smallest critical point and the smallest positive fixed point of  $F$ , respectively.

The two above mentioned mechanisms are well known and have been rigorously explained (see, e.g., [14]); however, we have found a different situation. For  $c = 0.47$ ,  $\gamma = 8.5$ , essential extinction would be expected to begin at  $\sigma = \sigma_1 \approx 0.86$ , when  $F^2(c_1) = q$ . However, at a previous value  $\sigma = \sigma_2 \approx 0.8315$ , an attracting 3-cycle disappears in a tangent bifurcation for  $F^3$ , in such a way that the transition from bistability to essential extinction occurs at  $\sigma = \sigma_2$  (see Figure 4.3, (c) and (d)).

The three examples shown in Figure 4.3 illustrate that there are multiple possibilities for the transition to extinction or essential extinction in equation (1.2).

**4.4. Extinction windows.** The influence of parameter  $\gamma$  on the dynamics of (1.2) is quite interesting, as it can be observed in the two-parameter diagram in Figure 4.1 for  $c = 0.47$ . For small values of  $\sigma$ , there is a transition from global stability of the positive equilibrium to bistability as  $\gamma$  passes the critical value  $\gamma = 1$ . This dynamical change occurs after a pitchfork bifurcation, where a new branch of (unstable) fixed points is born; see [8], where this bifurcation is explained for the gamma-Ricker map, which corresponds to (1.2) with  $\sigma = 1$ . This case is shown in Figure 4.4 (a) for  $\sigma = 0.05$ .

For larger values of  $\sigma$ , there are extinction windows, which were also observed in other models with Allee effects [6, 14, 15]. A simple extinction window originated by two tangent bifurcations as  $\gamma$  is increased (two positive equilibria disappear at the first one, but are created again in the second one) is shown in Figure 4.4 (b) for  $\sigma = 0.1$ . Since the map  $F$  governing the dynamics of (1.2) is bimodal for larger values of  $\sigma$  (see Theorem 2.1), there can be multiple extinction windows, as it has been reported in [6] for a population model with harvesting also governed by a bimodal map. These complicated dynamics are shown in Figure 4.4 (c) for  $\sigma = 0.9$ . Thus, a thorough analysis of the influence of  $\gamma$  on the dynamics of (1.2) in the parameter region where oscillations and essential extinction can occur seems to be a very difficult task.

It is worth noticing that, in some population models,  $\gamma$  is a cooperation parameter [2, 4], and extinction windows are related to a kind of “rescue effect”. That is to say, populations that go to extinction when cooperation rates are small can persist at intermediate population levels due to high cooperation intensity. However, larger rates of cooperation can lead to chaos and essential extinction. For related discussions, see [7, 8].

**5. Discussion.** Some months ago, the first author contacted Dr. P. J. Mitkowski to discuss about a model of delay differential equations for blood cell production, and he sent us a copy of the paper [5]. In this paper, published by Lasota in 1977, the beautiful equation (1.2) was proposed as a simple one-dimensional discrete-time model for the production of blood cells. To explain the influence of the destruction rate  $\sigma$  on the behavior of the solutions of (1.2), Lasota fixed  $c = 0.47$  and  $\gamma = 8$ .

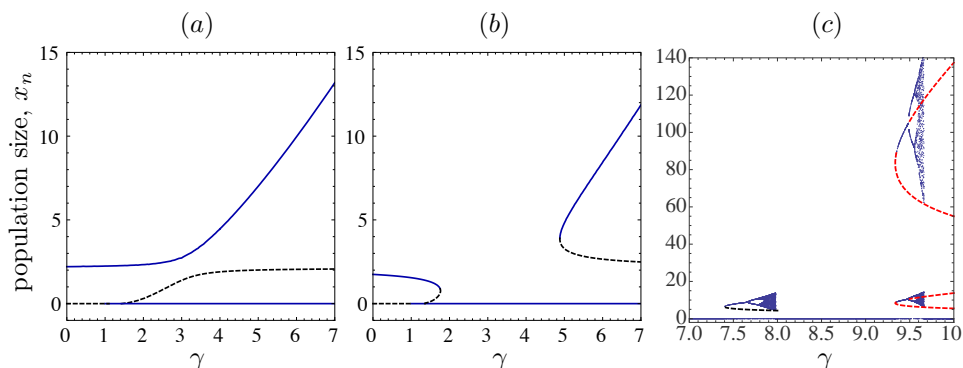


FIGURE 4.4. Bifurcation diagrams for equation (1.2) with  $c = 0.47$  and different values of  $\sigma$ , using  $\gamma$  as the bifurcation parameter. Black dashed lines correspond to unstable equilibria, and red dashed lines to unstable 2-periodic orbits. (a): There are neither oscillations nor extinction windows for  $\sigma = 0.05$ . (b): An extinction window for  $\sigma = 0.1$ . (c): Multiple extinction windows for  $\sigma = 0.9$ .

Then, he considered three values of  $\sigma$ , which were enough to explain the dynamics of blood cell production in some relevant clinical cases.

Our main motivation to write this paper was to carry out a much more detailed analysis of the dynamics of (1.2). We have combined an analytical study in Sections 2 and 3 with a numerical approach in Section 4. While in the latter section we have fixed  $c = 0.47$  as in [5], our theoretical results (Theorems 2.1, 3.1, 3.3 and Corollary 3.5) show the strong influence of  $c$  on the dynamics. In particular, very small values of  $c$  lead the system to extinction (see Figure 3.1).

The main purpose of Lasota in [5] was showing chaotic behavior in some biological models, including (1.2); this fact explains the choice  $\gamma = 8$  in [5]. Indeed, Figure 4.1 shows that if  $c = 0.47$  and  $\gamma < 7.5$ , then the dynamics of (1.2) is much simpler, as illustrated in Figure 4.3 for  $\gamma = 7$ .

The three cases studied in [5] correspond to  $c = 0.47$  and  $\gamma = 8$ , which are the parameters used in Figure 4.3 (b). We are in a position to discuss these cases in more detail. Lasota distinguished three situations:

1. Normal conditions in blood cell production are assumed to correspond to small values of  $\sigma$  ( $\sigma = 0.1$  in [5]). In this case, the number of blood cells tends to remain constant, but the organism dies if the number of cells is too small. This situation corresponds to the case when (1.2) has three equilibria  $0 < q < p$ , and 0 and  $p$  are asymptotically stable. In this example, this occurs for  $\sigma \in (0, \sigma_1)$ , where  $\sigma_1 \approx 0.331$  is the value at which  $p$  loses its asymptotic stability after a period-doubling bifurcation.
2. Intermediate values of  $\sigma$  would lead to a (non-severe) disease. For  $\sigma = 0.4$ , Lasota observed a 2-periodic attractor, explaining some oscillations in the number of blood cells that are typical of such diseases. The 2-periodic attractor corresponds to  $\sigma$  in the interval  $(\sigma_1, \sigma_2) \approx (0.331, 0.651)$ .

An interesting remark of Lasota is that the ill system is able to adapt to a larger destruction rate, because the average value of the 2-periodic orbit for  $\sigma = 0.4$  (about 13.1) is not much worse than the value of the attracting

positive equilibrium (about 15.4) for  $\sigma = 0.1$ . Actually, we observe a hydra effect, characterized by the fact that the average population can even increase as  $\sigma$  increases. For example, the average is 13.05 for  $\sigma = 0.33$ , and 13.074 for  $\sigma = 0.5$  (see the thick red line in Figure 4.3 (b)).

3. Larger values of  $\sigma$  in Lasota's example lead to chaotic behavior. The typical route of period-doubling bifurcations to chaos is observed in Figure 4.3 (b), (c). Lasota used the value  $\sigma = 0.8$ , for which a 3-periodic orbit can be found, and he reported a bistability scenario: solutions starting from an invariant interval  $[A, B]$  converge to the chaotic attractor, while solutions starting at an initial point  $x_0 \in (0, A)$  converge to zero. However, he did not mention that the basins of attraction of these two attractors collide at a larger value  $\sigma \approx 0.87$ , leading the population of cells to essential extinction.

One of the main conclusions of Lasota's example is that increasing  $\sigma$  is destabilizing. However, this is not always the case: our results show that a *bubbling* phenomenon is possible. For example, in Figure 4.2 we observe that the larger positive equilibrium  $p$  is asymptotically stable for  $\sigma = 0.9$  but unstable for  $\sigma = 0.7$ . Figure 4.3 (c) shows that the chaotic behavior can also be reversed by moving  $\sigma$  to a larger value. We refer the interested reader to [11] for further details and relevant references on bubbling.

Another interesting aspect not covered by Lasota's paper [5] is the influence of parameter  $\gamma$  in the dynamics of (1.2). Although the meaning of this parameter was not explained in [5], for a related model, Mitkowski [12] argued that  $\gamma$  can be interpreted as the degree of disturbance from the normal response in the feedback loop that regulates the production of cells in the bone marrow: when  $\gamma = 0$ , the answer is correct, but when  $\gamma > 0$ , the response is inhibited and the greater is the inhibition, the greater is the value of  $\gamma$ . For example, extinction is not possible for  $\gamma < 1$  (see Remark 3.2). For  $\gamma > 1$ , the dynamics strongly depend on the interaction between  $\sigma$  and  $\gamma$ : while for small values of  $\sigma$  changes in  $\gamma$  do not affect the dynamics, for larger values of  $\sigma$  there are extinction windows which can alternate with chaotic attractors (see Figure 4.4).

To finish, we emphasize that equation (1.2) is also of interest in population dynamics. When  $\sigma = 1$ , (1.2) is equivalent to the gamma stock-recruitment model used in fisheries [13], and has been also used in other contexts such as cooperation interactions in a group of individuals [2] and populations with Allee effects [4]. An important feature of this model is its flexibility, allowing different forms of density dependence (compensatory, overcompensatory, depensatory). For recent results and discussions in this direction, see [7, 8, 9]. In this context, equation (1.2) is a relevant generalization of the classical Ricker model.

On the one hand, the usual discrete-time models with Allee effects assume that adults cannot survive the reproductive season [15], but this assumption is not realistic for many populations. The introduction of a positive adult survivorship rate  $1 - \sigma$  ( $0 < \sigma < 1$ ) increases the generality of the model and induces some new dynamical phenomena in comparison with the classical gamma model. The most relevant are hydra effects, period-doubling reversals (bubbling), multiple extinction windows, and new mechanisms leading to essential extinction.

On the other hand, although the Ricker model with adult survivorship (corresponding to (1.2) with  $\gamma = 1$ ) has been considered before (see, e.g., [6, 11, 17] and references therein), the introduction of parameter  $\gamma$  makes the model more flexible. For example, Yakubu *et al.* showed that equation (1.2) with  $\gamma = 1$  fits well the

Atlantic cod fishery data, but the Pacific halibut data are best fitted with  $\gamma = 2$ . For  $\gamma > 1$ , the recruitment function  $f(x) = (cx)^\gamma e^{-x}$  combines both negative and positive density dependence. The parameter  $\gamma$  represents the strength of cooperation, and its influence on the stability and the size of the positive equilibria has been studied in [8].

The above discussion highlights the importance of studying equation (1.2) in the framework of population dynamics. In particular, for  $\gamma > 1$ , our analysis points out the subtle interplay between adult survivorship rates and Allee effects.

**Acknowledgments.** The authors thank Dr. Paweł J. Mitkowski for providing the crucial reference [5], and two anonymous referees for their useful comments on a first version of this paper. Eduardo Liz acknowledges the support of the research grant MTM2017–85054–C2–1–P (AEI/FEDER, UE). The research of Cristina Lois-Prados has been partially supported by the grant ED481A–2018/080 from Xunta de Galicia, and by grant MTM2016–75140–P (AEI/FEDER, UE).

#### REFERENCES

- [1] P. A. Abrams, [When does greater mortality increase population size? The long story and diverse mechanisms underlying the hydra effect](#), *Ecol. Lett.*, **12** (2009), 462–474.
- [2] L. Avilés, [Cooperation and non-linear dynamics: An ecological perspective on the evolution of sociality](#), *Evol. Ecol. Res.*, **1** (1999), 459–477.
- [3] E. Braverman and E. Liz, [Global stabilization of periodic orbits using a proportional feedback control with pulses](#), *Nonlinear Dynam.*, **67** (2012), 2467–2475.
- [4] F. Courchamp, L. Berec and J. Gascoigne, *Allee Effects in Ecology and Conservation*, Oxford University Press, New York, 2008.
- [5] A. Lasota, [Ergodic problems in biology](#), *Asterisque*, **50** (1977), 239–250.
- [6] E. Liz, [Complex dynamics of survival and extinction in simple population models with harvesting](#), *Theor. Ecol.*, **3** (2010), 209–221.
- [7] E. Liz, [A new flexible discrete-time model for stable populations](#), *Discrete Contin. Dyn. Syst. Ser. B*, **23** (2018), 2487–2498.
- [8] E. Liz, [A global picture of the gamma-Ricker map: A flexible discrete-time model with factors of positive and negative density dependence](#), *Bull. Math. Biol.*, **80** (2018), 417–434.
- [9] E. Liz and S. Buedo-Fernández, [A new formula to get sharp global stability criteria for one-dimensional discrete-time models](#), *Qual. Theory Dyn. Syst.*, (2019), 1–12.
- [10] E. Liz and D. Franco, [Global stabilization of fixed points using predictive control](#), *Chaos*, **20** (2010), 023124, 9 pp.
- [11] E. Liz and A. Ruiz-Herrera, [The hydra effect, bubbles, and chaos in a simple discrete population model with constant effort harvesting](#), *J. Math. Biol.*, **65** (2012), 997–1016.
- [12] P. J. Mitkowski, *Chaos in the Ergodic Theory Approach in the Model of Disturbed Erythropoiesis*, Ph.D. Thesis, AGH University of Science and Technology, Cracow, 2011.
- [13] T. J. Quinn and R. B. Deriso, *Quantitative Fish Dynamics*, Oxford University Press, New York, 1999.
- [14] S. J. Schreiber, [Chaos and population disappearances in simple ecological models](#), *J. Math. Biol.* **42** (2001), 239–260.
- [15] S. J. Schreiber, [Allee effects, extinctions, and chaotic transients in simple population models](#), *Theor. Popul. Biol.*, **64** (2003), 201–209.
- [16] M. Wazewska-Czyżewska and A. Lasota, [Mathematical problems of the red-blood cell system](#), *Mat. Stos.*, **6** (1976), 25–40.
- [17] A. A. Yakubu, N. Li, J. M. Conrad and M. L. Zeeman, [Constant proportion harvest policies: Dynamic implications in the Pacific halibut and Atlantic cod fisheries](#), *Math. Biosci.*, **232** (2011), 66–77.

Received January 2019; revised March 2019.

*E-mail address:* [eliz@dma.uvigo.es](mailto:eliz@dma.uvigo.es)

*E-mail address:* [cristina.lois.prados@usc.es](mailto:cristina.lois.prados@usc.es)